

EXPERIMENTAL INVESTIGATION ON THE SEISMIC RESPONSE OF BRIDGE BEARINGS

Dimitrios Konstantinidis¹, James M. Kelly² and Nicos Makris³

ABSTRACT

This paper contains the findings of an experimental study on the seismic response of three types of standard bridge bearings: (a) steel-reinforced elastomeric bearings, (b) steel-reinforced elastomeric bearings with PTFE disks, and (c) PTFE spherical bearings. The experimental program which was conducted partly at UC San Diego and partly at UC Berkeley included cyclic tests at various velocities and displacements for which these bearings have not been designed but may experience during an earthquake. The primary conclusions of these tests are that elastomeric bridge bearings perform exceptionally even under seismic loading conditions, accommodating well beyond the 50% limit proposed by current design guidelines for non-seismic conditions. PTFE-elastomeric bearings perform adequately but cannot accommodate rotations reliably. Spherical bearings featuring general-purpose adhesives perform very poorly under seismic conditions; however, when high-temperatures adhesives are used in their construction, these bearing perform very well under seismic conditions.

INTRODUCTION

Bridge bearings allow the translation and rotation of a bridge while carrying its gravity load to the substructure and foundation. They are capable of accommodating translations and rotations by using a variety of materials, most typically highly flexible elastomers or low-friction sliding surfaces. The type of bearing to be used is selected on the basis of load and displacement demands, site conditions, cost, and other factors. Elastomeric bridge bearings require little maintenance, have no moving parts, have good longevity and are very economical. Spherical sliding bearings can accommodate larger vertical loads, displacements and rotations but are considerably heavier and more expensive.

It is the purpose of this paper to describe a series of experimental studies of the seismic behavior of three types of standard thermal expansion bearings for bridges. The experimental program has used the Seismic Response Modification Device (SRMD) Testing System at the University of California, San Diego, as well as the testing facilities at the Pacific Earthquake Engineering Research (PEER) Center, University of California, Berkeley. The three types of bearings examined by the test program are

- 1) Steel-Reinforced Elastomeric Bearings,
- 2) Steel-Reinforced Elastomeric Bearings with PTFE Disks, and
- 3) PTFE Spherical Bearings.

¹ Dept. of Civil and Environmental Engineering, University of California, Berkeley

² Dept. of Civil and Environmental Engineering, University of California, Berkeley

³ Dept. of Civil Engineering, University of Patras, Greece

The test program includes wide-range dynamic tests at velocities and displacements that could be experienced by these bearings but for which they have not been designed.

ELASTOMERIC BRIDGE BEARINGS

For the purposes of this experimental study, a set of laminated elastomeric bridge bearing pads were manufactured by Scougal Rubber Corporation to Caltrans specifications. The set included six pads of three different sizes. This type of bearing is designed for a variety of deformations produced by thermal expansion of the bridge superstructure, shrinkage due to aging or prestress, misalignment or beam rotation. Under currently accepted design practice (AASHTO 1998, Caltrans 2000), the maximum shear strain developed in the elastomer due to all sources of deformation is not to exceed 50%. On the other hand, seismic isolation bearings for bridges and buildings are designed for much larger shear strains, and it is known that under shear loading the shear strain at failure can exceed 400%. This raises the issue that bridge-bearing specifications may be excessively conservative.

Bearing Design and Properties

Three pairs of plain elastomeric pads were designed for the test program with total rubber thicknesses of 48 mm, 120 mm, and 204 mm. The bearings had the same individual rubber layer thickness (12 mm), steel-shim thickness (1.9 mm), cover thickness (6 mm) and footprint dimensions (375 mm by 575 mm), but differed in the number of rubber layers and shims. Also the top and bottom layers were half the thickness of intermediate rubber layers, i.e., 6mm. These bearings did not have thick steel end plates like seismic isolation bearings. The rubber compound was Neoprene (polychloroprene) with a specified hardness of 55 on the Shore A Scale. The steel shims were A1011 steel. Table 1 shows detailed geometric properties of the bearings. The bearings were manufactured by Scougal Rubber Corporation to comply to ASTM D4014 (Standard Specification for Plain and Steel-Laminated Elastomeric Bearings for Bridges) as required by Caltrans (2000).

Table 1. Geometric characteristics of the steel-laminated elastomeric pads.

Bearing designation	Rubber height [mm (in.)]	No. of steel shims	Total height [mm (in.)]	Width [mm (in.)]	Depth [mm (in.)]
S-48	48 (1.89)	4	55.6 (2.19)	375 (14.76)	575 (22.64)
S-120	120 (4.72)	10	139.0 (5.47)	375 (14.76)	575 (22.64)
S-204	204 (8.03)	17	236.3 (9.30)	375 (14.76)	575 (22.64)

Test Program

The test program on the elastomeric pads, which was conducted at UC San Diego’s SRMD testing facility, included a number of sinusoidal input signals varying in frequency and amplitude. The tests were conducted under a high vertical load of 401 kips (corresponding to an average pressure of 1200 psi) and a low vertical load of 67 kips (200 psi). The direction of loading was parallel to the short dimension of the bearing, as they are expected to be loaded in a

bridge. The pads were tested with 0° rotation as well as with a 1.5° rotation about the horizontal axis transverse to the loading axis. This imposed rotation was intended to replicate the in-situ boundary conditions where the bridge girder supported by the bearing may be rotated. 10- and 50-cycle serviceability tests at shear strains up to 50% and frequencies up to 0.33 Hz were conducted. Seismic loading conditions were replicated by 3-cycle signals with various amplitudes ranging from 100% up to 300% shear strain and velocities up to 32 in/sec. For each pad, the tests were carried no further than the shear strain that would result in the originally vertical face becoming horizontal.

Experimental Findings on the Seismic Response of Elastomeric Bearings

The experiments show that the elastomeric bridge bearings perform exceptionally even under seismic loading conditions. The bearings were able to withstand very large shear strains without any damage, which reinforces the idea that present design guidelines for bridge bearings that limit the combined shear strains to 50% may be overly conservative. Elastomeric bridge bearings have relatively thin steel reinforcing plates compared to seismic rubber isolators. This flexibility and the absence of thick steel end-plates allows the unbonded surfaces to roll off the loading surfaces when the bearing is sheared, as shown in Fig. 1, thus relieving the tensile stresses that would otherwise be produced if the top and bottom surfaces of the bearing were bonded to the supports.



Fig. 1. The corners of the S-204 elastomeric bearing rolling off the top and bottom supports as the bearing is sheared in the direction pointed by the arrows.

The experimental results show that the roll-off response is limited by the fact that the free edge of the bearing rotates from the vertical towards the horizontal with increasing shear displacement, and the limit of this process is reached when the originally vertical surfaces at each side come in contact with the horizontal surfaces at both top and bottom (i.e., *roll-over*). Further horizontal displacement beyond this point can only be achieved by slipping. Slip can produce damage to the bearing through tearing of the rubber, distortion of the reinforcing steel, and heat generated by the sliding motion. Thus the ultimate displacement for an unbonded bearing of this type can be specified as that which transforms the vertical free edge to a horizontal plane. Determining analytically the ultimate shear strain is very complicated, but a lower bound of the ultimate shear strain can be obtained if certain assumptions are made (Konstantinidis et al. 2008).

The value of horizontal stiffness for bonded bearings is estimated using the familiar formula $K_H = GA/t_r$, where G is the shear modulus, A is the plan area of the bearing, and t_r is the total

thickness of the rubber. The horizontal force is given by $F_s = K_H \Delta = GA\Delta/t_r = GA\gamma$, where $\gamma = \Delta/t_r$ is the shear strain. For unbonded bearings, this formula is applicable only under low shear strains because they tend to roll off the top and bottom support at larger shear strains. It was observed that the stiffness value estimated by the above formula deviates from the experimentally determined value more as the thickness of the bearing increases. This is attributed to the fact that for a taller bearing, a shear strain γ_o corresponds to a larger horizontal displacement and, therefore, a larger reduction in effective shear area due to the roll-off effect than for a shorter bearing.

The study examined the effect of the displacement amplitude on the shape of the hysteretic loops for the S-48, S-120 and S-204 bearings. For the S-48 bearing, the shape of the hysteretic loop is not affected as the displacement increases. This is because the height-to-width ratio of the bearing is small. Only for the test with 300% imposed shear strain, for which sliding was observed, does the hysteretic loop shape change. On the other hand, for the S-120 and S-204 bearings which have larger height-to-width ratios, the effect of the roll-off becomes apparent on the hysteresis loops as the imposed displacement is increased. This effect is more pronounced under lower pressure.

The experiments showed that the energy dissipated per cycle, EDC , is nearly independent of velocity. The areas of individual hysteresis loops of experiments conducted under the same pressure and at the same shear strain level but at different loading rates are approximately equal, indicating that the energy dissipated per cycle is independent of loading rate. This behavior is observed for all tests on the S-48 bearing and for most tests on the S-120 and S-204 bearings. Some velocity dependence is observed for the S-120 bearing under the low pressure (200 psi) at 150% shear strain and for the S-204 bearing under the low pressure (200 psi) at 100% shear strain. In these cases, the EDC increases with velocity. The general observation from these experiments that the EDC is fairly rate-independent confirms that damping in rubber and rubber-like materials is predominantly hysteretic, not viscous. Finally, there is generally an increase in the EDC with increasing vertical load for all bearings tested.

Current design guidelines ignore the roll-off effect and assume a Coulomb friction behavior on the support interface. The force is given by $F_s = GA\gamma \leq \mu P$, where μ is the friction coefficient, and P is the compressive force on the bearing. In reality, as the bearing is sheared, it rolls off the supports, and the effective area of the bearing decreases. Consequently, the horizontal stiffness of the bearing decreases, and the behavior is not linear. If the bearing is stocky (small height-to-width ratio), like the S-48 bearing, the effect of the roll-off is not pronounced, and eventually, once a limiting force is reached, the bearing begins to slide. From the experiments, it was observed that this limiting force was reached when the S-48 bearing rolled over. As the height-to-width ratio of the bearing increases, however, the reduction in effective area due to roll-off becomes very important; and if the bearing is tall enough, the load displacement curve begins to descend before the force reaches the limiting force to start sliding. On the descending part of the load-displacement curve, the bearing is unstable.

To account for the reduction in area due to roll-off, an effective (or reduced) area can be used, giving $F_s = GA\gamma(1 - \lambda\gamma)$, where $\lambda = t_r/(2b)$ (Konstantinidis et al. 2008). The effective stiffness is $K_H = (GA/t_r)(1 - 2\lambda\gamma)$, which suggests that the tangent stiffness of the bearing is zero when

$\gamma = b/t_r$. It should be noted that this estimate is a lower bound to the value of strain that causes zero tangent stiffness since in estimating the reduced area the small bending stiffness of the steel shims is ignored. In the case of these bearings, this shear strain is 3.92 for S-48, 1.56 for S-120, and 0.92 for S-204. Experimentally, for the S-204 bearing, the zero-stiffness (maximum force) point occurs at roughly 85-90% shear strain. Clearly, roll-off is of no importance in stocky bearings but very significant for the slender bearings. For stocky bearings (S-48), the design displacement must not exceed the roll-over displacement, while for slender bearings (S-204), the design displacement must not exceed the displacement after which the load-displacement curve begins to descend. For bearings with intermediate height-to-width ratio, both criteria must be checked; the design displacement must be less than the lower of the two displacement limits. Experimentally and analytically obtained shear strain limits and force-displacement curves for the three elastomeric bearings used in this study are offered in Konstantinidis et al. (2008). That report also presents graphs of maximum horizontal force versus peak shear strain obtained by best-fitting the test results under different compressive loads, rotations and loading directions. The tests showed that maximum horizontal force is nearly frequency-independent at a fixed compressive load, and therefore the results can be expressed by a single load-shear strain curve.

In the single test where sliding was observed, it was noted that the force increases until roll-over. After roll-over occurred, the test machine continued to push the bearing although no further shear deformation was possible, and the increased displacement resulted in slippage. The force continued to increase after roll-over, which means that the slip process is not simple Coulomb friction (i.e., no constant force during slipping), but rather it includes a degree of adhesion.



Fig. 2. Damage caused on the S-48 bearing when it was sheared beyond the limit of the originally vertical edges becoming horizontal (300% shear strain, 1200 psi pressure).

In some cases the F_s / P ratio exceeded the frictional coefficient values recommended in existing Caltrans guidelines (Caltrans 1994) even if the bearing did *not* slide. These guidelines suggest that the friction is the Coulomb type and recommend the use of a friction coefficient of 0.40 for concrete to rubber and 0.35 for steel to rubber. From the experiments, the maximum F_s / P under $P = 67$ kips compressive load was around 0.53 at 184% strain (without slipping occurring). Therefore, the horizontal load that can transfer to the substructure exceeds $0.53 \cdot 67$ kips. The F_s / P ratio observed under $P = 67$ kips exceed in several occasions the recommended value of 0.4. Therefore, for bearings under low design pressure (200 psi), the recommended value for friction coefficient may need to be increased in future design guidelines. On the other hand, for

$P = 401$ kips, the maximum F_s / P ratio obtained was 0.35. Therefore, for bearings under large design pressure (1200 psi), the recommended values were not exceeded.

Another issue of concern was the ability of the bearings to accommodate rotations. The S-120 and S-204 bearings were visibly able to accommodate the 1.5-degree rotation; the S-48 bearing, however, was too stiff in bending to do so under the 67-kip compressive load without leaving a gap on the contact interface. Under the 401-kip compressive load, this gap was diminished. The experimental results show that the measured K_H and F_s / P are slightly reduced for the rotated tests on the S-48 bearing. The rotation appears to have a negligible effect on the EDC . The same pattern is observed for the S-120 bearing as for the short bearing although it is less pronounced. The same can be concluded for bearing S-204.

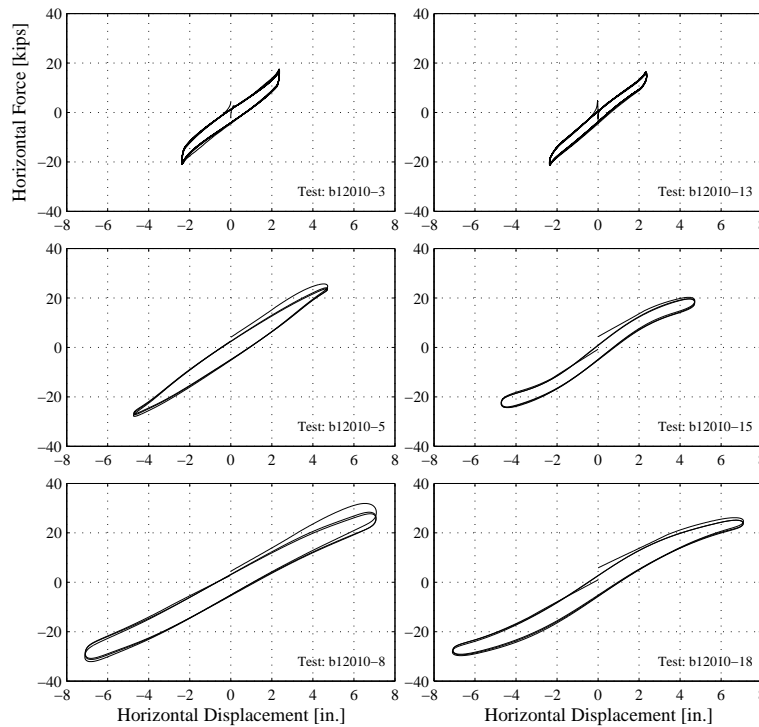


Fig. 3. Evolution of hysteretic loops as the displacement increases for the S-120 bearing under an average pressure of 1200 psi (left) and 200 psi (right).

PTFE-ELASTOMERIC BRIDGE BEARINGS

This phase of the experimental program included testing at UC San Diego of a set of PTFE-elastomeric bridge bearings manufactured to Caltrans requirements by Scougal Rubber Corporation. These bearings are designed and used solely as thermal expansion bearings, but the purpose of this study is to determine their response under seismic conditions.

Bearing Designs

Fig. 4 shows the two PTFE-elastomeric bearings tested in this study. The bearing consists of an elastomeric pad (identical to those described in the previous section) that is bonded to thick

A36/A36M steel end plates on top (*intermediate plate*) and bottom (*masonry plate*). Typically, the recommended thickness of the masonry plate is 0.75 in., while the thickness of the intermediate plate is determined by the designer in accordance to the AISC design procedures for column base plates. The intermediate plate features two PTFE disks manufactured from 100 percent pure virgin unfilled dimpled sheet resin. These disks are in contact with a *sole plate*. The sole plate is made of A36/36M steel that has stainless steel surfacing, which provides the sliding surface for the PTFE disks. The rubber compound on the elastomeric part of the bearing is Neoprene (polychloroprene) with a hardness of 55 (shore). Each intermediate rubber layer is 12 mm thick, while the top and bottom rubber layers are 6mm thick. The bearings are laminated with 14-ga (1.9 mm) A1011 steel shims. Table 2 lists the geometric features of the PTFE-elastomeric bearings.

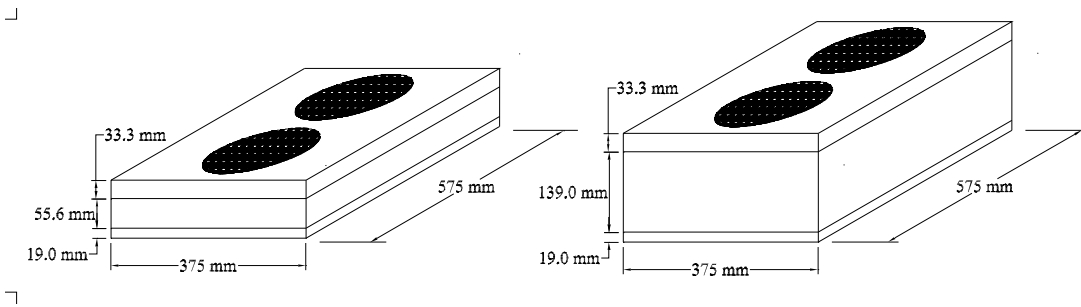


Fig. 4. The two PTFE-elastomeric bearings.

Table 2. Geometric characteristics of the steel-laminated elastomeric pads.

Bearing designation	No. of rubber layers	Total rubber height [mm (in.)]	No. of shims	PTFE disks (2) [mm (in.)]	Sole Plate $H \times W \times D$ [mm (in.)]	Inter. Plate $H \times W \times D$ [mm (in.)]	Masonry Plate $H \times W \times D$ [mm (in.)]
S-48	3 + $2 \times \frac{1}{2}$	48 (1.89)	4	6 × f200 (0.236 x f7.87) recessed 3mm	25 × 900 × 850 (0.984 × 35.43 × 33.46)	35 x 375 x 575 (1.38 x 14.76 x 22.64)	20 x 375 x 575 (0.79 x 14.76 x 22.64)
S-120	9 + $2 \times \frac{1}{2}$	120 (4.72)	10	6 × f200 (0.236 x f7.87) recessed 3mm	25 x 900 x 850 (0.984 x 35.43 x 33.46)	35 x 375 x 575 (1.38 x 14.76 x 22.64)	20 x 375 x 575 (0.79 x 14.76 x 22.64)

The idea behind these bearings is that the elastomeric part will accommodate rotations, while horizontal movements will be accommodated by the low friction sliding interface between the PTFE and stainless steel. In order for the bearings to accommodate rotations, their bending stiffness has to be low. The shape factor of the bearing has to be kept low if the bearing is to be effective in accommodating rotations. Differential rotation between the superstructure and the bearing may result in gouging of the stainless steel plate by the edge of the intermediate plate. This was indeed the case for the bearings that were tested. The original test protocol included tests to be conducted at 1.5-degree rotation. However, it was noted during preparation for the tests that the bearings were not able to accommodate this rotation. The T-120 bearing was barely able to accommodate a 0.5 degree rotation, and the T-48 bearing could only accommodate a

fraction of this. To prevent gouging of the stainless steel plate, it was decided to test the 48-mm bearing only unrotated.

Test Program

The test program on the PTFE-elastomeric bearings included a number of sinusoidal input signals varying in frequency and amplitude. The tests were conducted under a high vertical load of 401 kips, which corresponds to 1200 psi average pressure on the elastomer and 4117 psi on the PTFE. 1200 psi is the maximum average pressure allowed on the elastomer in current practice, and 200 psi is the minimum. A low vertical load of 195 kips, which corresponds to 580 psi average pressure on the elastomer and 2,000 psi on the PTFE. By specification, 2,000 psi is the minimum average pressure allowed on the PTFE (the maximum is 3,500 psi). Bearing T-120 was tested with a 0-degree rotation as well as with a 0.5-degree rotation about the axis transverse to the loading axis. Bearing T-48 was tested only with a 0-degree rotation.

To assess the service behavior of the bearings, 10- and 20-cycle serviceability tests were conducted. To test the response of the bearings to seismic loading conditions, 3-cycle signals were used. For the T-48 bearing, the displacement amplitude of the signals ranged from 2 to 8 inches and the frequencies from 0.016 to 2.4 Hz. For the T-120 bearing, the displacement amplitude of the signals ranged from 6 to 12 inches and the frequencies from 0.005 to 0.8 Hz.

Experimental Findings on the Seismic Response of PTFE-Elastomeric Bearings

Fig. 5 plots the hysteretic loops for the T-48 bearing at zero rotation under a 401-kip compressive load. The input sinusoidal signal had displacement amplitude $u_o = 8$ in. and velocity amplitude $v_o = 30$ in/sec. The displacement plotted in the figure is that imposed by the testing machine actuators. It is equal to the sum of the displacement due to the deformation of the rubber and the displacement due to sliding on the PTFE disk. At small displacements, the rubber portion of the bearing accommodates the full displacement. As the bearing is sheared further, once the frictional resistance of the PTFE-steel interface is overcome, sliding occurs along the PTFE disks. Fig. 5 also shows some of the quantities of interest that characterize the response of these bearings.

Previous studies (e.g., Mokha et al. 1988) have noted that the frictional resistance of PTFE is sensitive to velocity and pressure. This study confirms this behavior. The kinetic friction coefficient μ for the T-48 bearing varied from as little as 0.02 to as much as 0.12. For the T-120 bearing at 0 degree rotation, varied between 0.03 and 0.08, while for the T-120 bearing the range was 0.02 to 0.09 at 0.5 degree rotation.

Fig. 6 plots μ as a function of velocity and pressure. It is important to note that here by *velocity* we mean the peak velocity (the amplitude) of the sine signal, *not* the instantaneous velocity. It is evident that for a given pressure, the friction coefficient is lower and more variable at low velocities. At higher velocities, μ is constant. It is lower for higher pressures, and the velocity-range in which it varies is smaller than for lower pressures. The friction coefficient of the T-120 bearing is slightly larger when the bearing is tested with rotation. This is most likely because the rotation imposes an uneven distribution of stress on the PTFE disks. The frictional resistance on the portion of the disk that is under lower pressure is larger, while the frictional resistance on the

portion that is under higher pressure is not effected as much. This results in a slightly higher measurement.

Fig. 6 also shows that the friction coefficient decreases with increasing pressure. This behavior is explained by Bowden and Tabor (2001).

The amount of displacement that is accommodated by the elastomeric portion of the rubber before sliding initiates at the PTFE-stainless interface is fairly independent of the loading rate and can be crudely estimated by $\Delta_r = \mu P t_r / (GA)$. Δ_r is larger when a bearing is under a larger compressive load. Although μ is smaller at larger pressures, the product μP which gives the strength of the interface is larger.

Excessive shedding of PTFE was observed during the experiments. The left photograph in Fig. 7 shows flakes of PTFE resulting from fast testing, and the photograph on the right shows the condition of the PTFE disks after completion of the tests. The reduction in thickness of the PTFE disks is visibly notable after testing, and the dimples around the edges of the disks are completely filled with particles that have shredded off. It is not clear if the excessive flaking affects the mechanical behavior of the PTFE-elastomeric bearings in the short term, although a slight reduction in the strength of the sliding interface that was noted with each successive cycle may be the result of this wear.

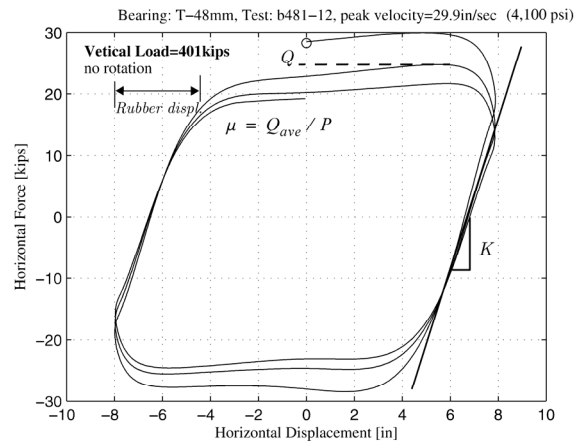


Fig. 5. Recorded hysteretic loops for a fast cyclic test on the T-48 bearing.

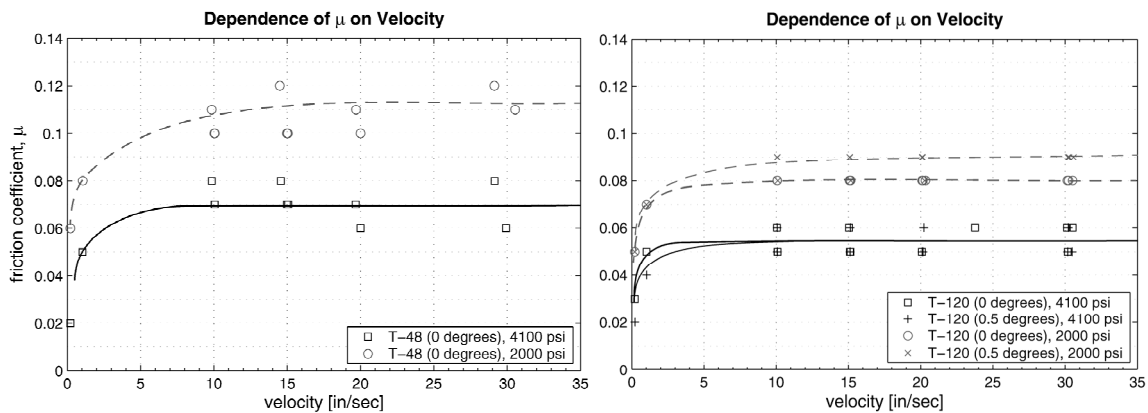


Fig. 6. Recorded hysteretic loops for a fast cyclic test on the T-48 bearing.



Fig. 7. Wear of PTFE during fast tests.

SPHERICAL BRIDGE BEARINGS WITH GENERAL-PURPOSE ADHESIVES

The first phase of the experimental program on spherical bearings was conducted at the Caltrans SRMD facility in UC San Diego. This included testing of a set of PTFE spherical bridge bearings manufactured to Caltrans requirements by Lubron Bearing Systems Corporation of Huntington Beach, CA. These bearings are designed and used as thermal expansion bearings but were tested in this study under seismic loading conditions. The steel-reinforced elastomeric bearings and the PTFE-elastomeric bearings described in the previous sections are much more commonly used as thermal expansion bridge bearings. These types of bearings however are not capable of accommodating large rotations. In applications where large rotations (even up to 3 degrees) need to be accommodated, spherical bearings are used.

Bearing Designs

The type of unguided spherical bearing tested is a Lubron *TF structural spherical* bearing. It consists of a woven PTFE fabric liner bonded to the carbon steel substrate. The PTFE fibers are interwoven with secondary glass fibers so that the PTFE is predominant near the sliding surface for minimum coefficient of friction, while the glass fibers are predominant near the bonded surface for maximum adhesion to the carbon steel. The construction of these bearings provides support of the individual PTFE fibers and ensures a rigid bond of the fabric to the substrate by using a general-purpose epoxy adhesive with high peel strength and high toughness. The adhesive is rated for temperatures up to 250°F (120°C). The design of these bearings allows rotations about any horizontal axis by sliding along a spherically shaped interface on one side of the bearing (Fig. 8, left). Large horizontal displacements of the superstructure can be accommodated by sliding along a flat woven PTFE sliding interface on the other side of the bearing (Fig. 8, right). Two identical bearings were manufactured for the purpose of this study. Each bearing was resurfaced with new woven-PTFE fabric on the horizontal surface several times during the course of the test program so as to provide a virgin surface to the extend practically possible.



Fig. 8. Left: convex plate. Right: concave plate resting on top of convex plate.

Test Program

The test program on the Lubron spherical bearings included a number of sinusoidal input signals varying in frequency and amplitude. The tests were conducted under various pressures ranging from 2,000 psi up to 10,000 psi. The bearings were tested both without rotation and with a 2-degree rotation. The 2-degree rotation was applied using a 2-degree wedge plate. To test the response of the bearings to loading conditions that would result from earthquake shaking, 3-cycle signals were used. These signals included half-cycle before and half-cycle after the main 3-cycle signal. The stroke was 2.5 and 5.0 inches. A limited number of 8.0 inch tests were also conducted. Note that the originally designed test protocol was not followed to completion for some of the bearings. This was due to excessive wear on the PTFE surface that made it necessary to suspend testing on the particular bearing until it was resurfaced with a new liner.

Experimental Findings on the Seismic Response of Spherical Bridge Bearings with General-Purpose Adhesives

Only two of the six specimens were able to survive the entire test protocol. One specimen experienced moderate damage, while three others experience significant damage after repeated testing, and testing on them was eventually suspended. The problem these bearings experienced was the tendency of the general-purpose epoxy adhesive to melt under high pressures and velocities, which resulted in the degradation of the PTFE sliding surface.

Fig. 9 plots hysteretic loops from a fast test. The hysteretic loops exhibit the typical behavior for a sliding system in the sense that there is a force overshoot at the initiation of sliding, yet they are different in that during sliding the force does not remain relatively constant, but rather it drops. The time histories show that the variation in friction force cannot be a function of velocity alone. The decrease in force observed while the slider is moving is due to heat generated by friction, which results in a decrease in the frictional resistance of the sliding interface.

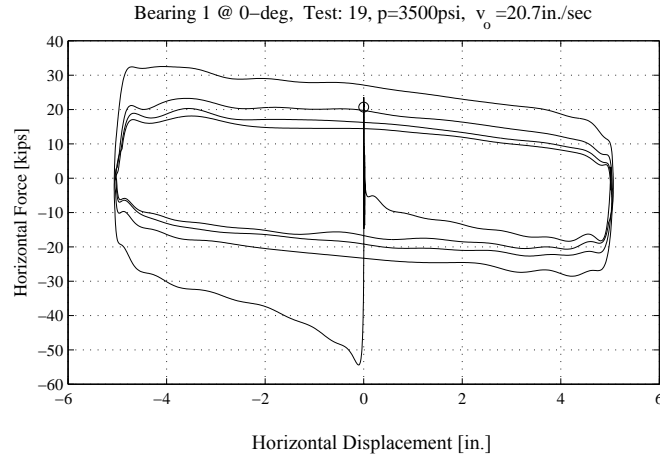


Fig. 9. Hysteretic loops for a 3-cycle test at a velocity amplitude of 20 in/sec.

Much of the test protocol was suspended due to damage on the woven PTFE liner and the stainless steel plate. The epoxy adhesive appeared to have exceeded its melting temperature of 250°F and baked onto the mating stainless steel sliding surface. Under normal conditions, microscopic particles of PTFE transfer and burnish onto the stainless steel, creating a low-friction sliding interface. During these tests, however, melted epoxy resin also adhered onto the sliding surface, resulting in a rougher interface which accelerated the wear and deterioration of the PTFE liner. Considerable effort using solvents and scouring pads was required to remove the fused epoxy resin from the sliding surface. Fig. 10 shows photographs of the damage on a specimen after the completion of the test protocol. The photograph on the left shows the flaking of the PTFE liner that resulted during testing. The center photograph shows the condition of the PTFE liner, which has deteriorated considerably. In a few locations at the edges running along the direction of motion, the PTFE appears to be completely worn out. The photograph on the right shows epoxy and PTFE that has fused onto the stainless steel surface.



Fig. 10. Left: PTFE flaking. Center: damaged woven PTFE liner. Bottom: fused epoxy and PTFE on the stainless steel surface.

SPHERICAL BRIDGE BEARINGS WITH HIGH-TEMPERATURE ADHESIVES

The tests conducted at the Caltrans SRMD Testing Facility in UC San Diego on full scale spherical bearings that featured PTFE sliding surfaces that were bonded using general-purpose adhesives identified a serious degradation problem. The underperformance of those bearings motivated an experimental investigation into the performance of PTFE liners which instead of a general-purpose adhesive use High-Temperature adhesives. Woven PTFE surfaces with two types of adhesives were investigated:

- 1) A high temperature resistant epoxy film adhesive with excellent bond strength. Excellent resistance to salt spray and high humidity. Suitable for temperatures up to 400°F (204°C). Surfaces using this High-Temperature *Epoxy* adhesive are referred to as HTE in this paper.
- 2) L-526 high temperature resistant phenolic prepreg adhesive with high peel strength and high toughness. Suitable for temperatures up to 500°F (260°C). Surfaces using this High-Temperature *Phenolic* adhesive are referred to as HTP in this paper.

Test Program

Seven sets (1 set = two plates) of woven PTFE bearing specimens were tested. Three sets featured HTE, three sets HTP and one set general-purpose adhesive. The specimens consisted of 6-in. square woven PTFE sliding surfaces bonded with the different type adhesives to 8×8×2 in. plates. The tested specimens did not feature a spherical part.

The experimental study was conducted at the Pacific Earthquake Engineering Research Center testing facility at Richmond Field Station, UC Berkeley. A 100-kip small-viscous-damper testing machine was modified to accommodate the PTFE bearing plates. Fig. 11 shows two photographs of the setup. The left photograph shows the modified testing machine. The crossbeam on the top is driven by the two 50-kip vertical actuators. The components of the setup that are painted black serve as a pedestal and a prestressing frame. The right photograph shows a close up of the 2-inch-thick bearing plates that feature the PTFE liner sandwiching a steel plate (referred to as the *stainless steel plate* henceforth) that features thin stainless steel sheets on either side. On the other side of each bearing plate there is a 2-inch backing plate. The bearing plates are fixed, while the stainless steel plate is driven up and down. The input signals were sinusoidal waves with 5 in. displacement amplitudes and with velocity amplitudes of 0.2, 1, 2, 5, 8, 11, 14, 17, 20, 25, 30, 40 in/sec. The actuators were able to perform very well at all but the highest velocities. At those velocities the desired velocity amplitude is not attained, and the produced signal deviates slightly from a sine wave. The 0.2 and 1 in/sec signals consisted of 10 cycles, while all other signals consisted of 3 full cycles plus one entry half-cycle and one exit half-cycle. The entry and exit half-cycles are smoothed so that the velocity signal starts and ends at zero.

The desired pressure on the PTFE is achieved by tuning the forces on four horizontal prestressing bars (see Fig. 11), which are monitored by four donut-type load cells. Tests were conducted at pressures of 2000, 3500, 5500, 7500 and 10000 psi. A load cell connects the stainless steel plate and the cross beam. The force measured by the load cell is the frictional resistance from the two sliding interfaces, one on each side of the stainless steel plate.

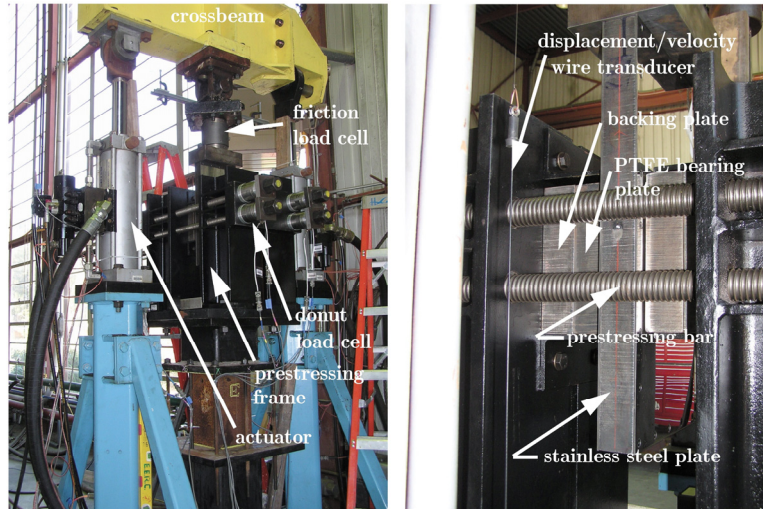


Fig. 11. Left: testing machine modified to accommodate the PTFE bearing plates. Right: close-up of the PTFE bearing plates sandwiching the stainless steel plate.

Experimental Findings on the Seismic Response of Spherical Bridge Bearings with High-Temperature Adhesives

Both the High-Temperature Epoxy and the High-Temperature Phenolic Adhesive PTFE bearings exhibited superior performance during the tests. Little shedding was noticed, and the adhesive did not appear to melt and bake onto the stainless steel, as it did in the tests performed on PTFE bearings with the General-Purpose Epoxy (GPE) adhesive at the SRMD testing facility in UC San Diego. For comparative purposes, a set of bearings using the same General-Purpose adhesive as the bearings at UC San Diego was tested. The heat generated by friction resulted in excessive degradation of the GPE PTFE liner. After only 10 tests, when the test with was run, a considerable amount of smoke surrounded the test setup, and at that point it was decided to discontinue testing on the GPE PTFE set of bearings. The left photograph of Fig. 12 shows the condition of the GPE bearing under 10 tests, while the right photograph shows the condition of one of the HTP bearings after completing the test protocol. The superior resistance of the latter to wear is obvious.

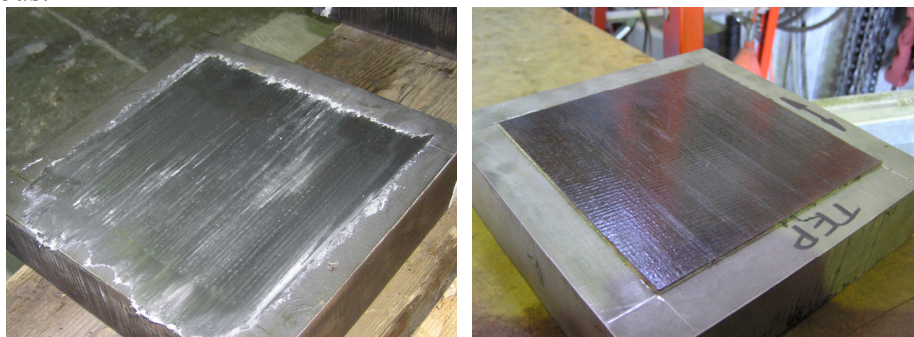


Fig. 12. Left: PTFE liner with general-purpose epoxy adhesive after 10 tests. Right: PTFE liner with high-temperature phenolic adhesive after completing the test protocol (60 tests).

Fig. 13 plots displacement, velocity and friction force histories on the left column for a typical fast test on a HTP bearing at an average pressure of 5500 psi and velocity amplitude of 22.4 in/sec. The top graph on the right column of plots the friction coefficient μ defined as the

recorded friction force divided by two (since there are two friction surfaces) divided by the instantaneous clamping (i.e., normal) force, versus the displacement. We note that the friction coefficient attains its maximum near the initiation of motion and is not constant thereafter. It varies as the velocity of the signal varies. Moreover, it decreases due to heat buildup along the sliding interface. The middle graph on the right column of the figure plots the average pressure versus displacement. We note that the average pressure does not deviate significantly from the preset value of 5500 psi. The bottom graph plots μ as a function of total distance travelled. This graph makes it easier to see how μ ever decreases due to heat buildup on the sliding surfaces as the total distance travelled increases.

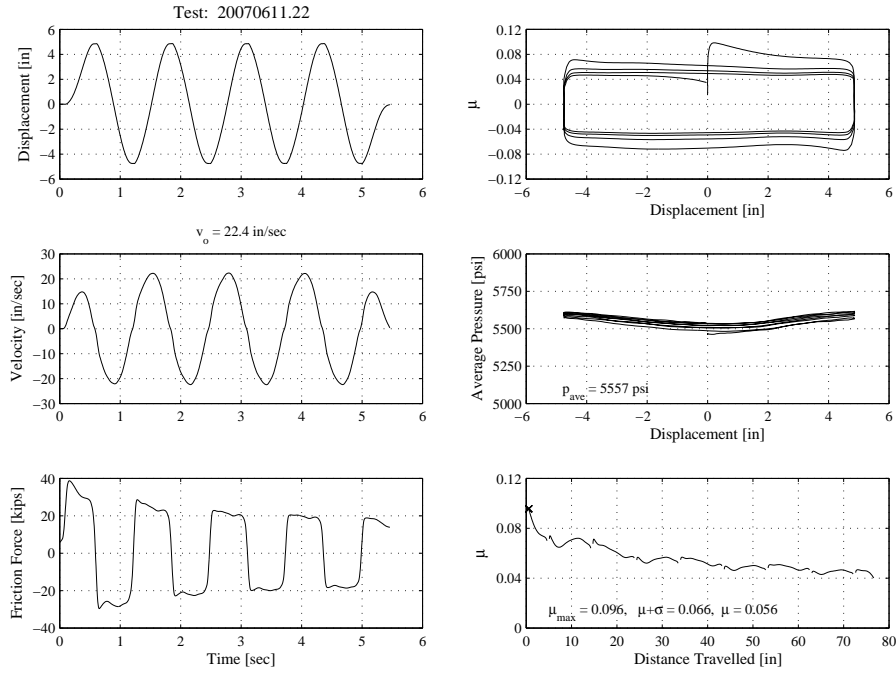


Fig. 13. Time histories and hysteresis loops for a typical fast test on a HTP PTFE bearing.

The variability of μ within each test made it necessary to present average, μ_{ave} , average plus one standard deviation, $\mu_{ave} + \sigma$, and maximum, μ_{max} . Also, the dependence of μ on velocity amplitude and pressure made it necessary to develop graphs and relationships under these different conditions (Konstantinidis et al. 2008). A typical such graph is shown in Fig. 14. The curves are obtained by fitting the experimental data to a 2-1 rational fit model that takes the form

$$\mu(v_o) = \frac{\alpha_1 v_o^2 + \alpha_2 v_o + \alpha_3}{v_o + \beta}$$

where v_o is the velocity amplitude of the forcing signal and $\alpha_1, \alpha_2, \alpha_3, \beta$ are fit parameters. Tables of these fit parameters for different pressures can be found in Konstantinidis et al. (2008).

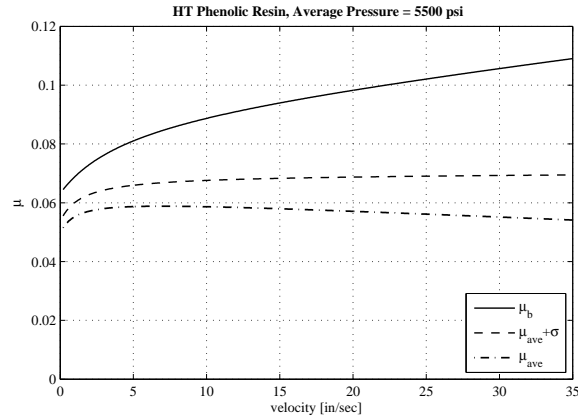


Fig. 14. Friction coefficients for HTP Woven-PTFE under 5,500 psi.

ACKNOWLEDGEMENTS

This work was supported by Caltrans under grant 59A0436.

REFERENCES

- AASHTO. 1998. *LRFD Bridge design specifications: SI units*. 2nd ed. American Association of State Highway and Transportation Officials. Washington, DC.
- Bowden F.P. and Tabor D. 2001. *The friction and lubrication of solids*. Oxford University Press, New York, NY.
- Caltrans. 1994. *Bridge memo to designers*. Section 7: Bridge Bearings. California Department of Transportation, Sacramento, CA.
- Caltrans. 2000. *Bridge design specifications*. Section 14: Bearings. California Department of Transportation, Sacramento, CA.
- Konstantinidis, D., Kelly, J.M. and Makris, N. 2008. *Seismic response of bridge bearings*. Report No. EERC-2008/02, Earthquake Engineering Research Center, University of California, Berkeley, CA.
- Mokha A., Constantinou M.C., and Reinhorn A.M. 1988. *Teflon bearings in aseismic base isolation: experimental studies and mathematical modelling*. Technical Report NCEER-88-0038. National Center for Earthquake Engineering Research. State University of New York at Buffalo, NY.